THE ASTROPHYSICAL JOURNAL SUPPLEMENT SERIES, 73:199–207, 1990 June

ION AND RELATIVISTIC ELECTRON TRANSPORT IN SOLAR FLARES

R. RAMATY
Laboratory for High Energy Astrophysics, Goddard Space Flight Center
J. A. MILLER AND X.-M. HUA
Department of Physics and Astronomy, University of Maryland, College Park
AND
R. E. LINGENFELTER
Center for Astrophysics and Space Sciences, University of California, San Diego
Received 1989 March 2; accepted 1989 June 23

ABSTRACT

We review recent models for ion and relativistic electron transport in solar flare magnetic loops. We discuss the depth distributions of gamma-ray production, the attenuation of gamma-ray lines, the time dependences of the various emissions, and the angular distribution of the bremsstrahlung.

Subject headings: gamma rays: general — hydromagnetics — particle acceleration — Sun: flares — Sun: particle emission

I. INTRODUCTION

The observations of gamma rays and neutrons from solar flares and their implications on particle acceleration and transport have been reviewed in several publications (e.g., Chupp 1984, 1987; Ramaty and Murphy 1987; Ramaty *et al.* 1988). Here we wish to discuss the recent results obtained from considerations of ion and relativistic electron transport in magnetized flare loop models (Zweibel and Haber 1983; Kocharov *et al.* 1987, 1988, Ramaty *et al.* 1988; Hua, Ramaty, and Lingenfelter 1989; MacKinnon and Brown 1989; Miller and Ramaty 1989).

That the bulk of the gamma rays observed from solar flares are produced inside closed magnetic structures is suggested by the comparison of the number of interacting protons, deduced from the gamma-ray observations, with the number of observed in interplanetary space from the same flare. This comparison shows that the interacting protons are generally more numerous than the escaping ones (von Rosenvinge, Ramaty, and Reames 1981; Murphy and Ramaty 1984), implying that the protons are efficiently trapped and forced to interact at the Sun. Because of the well-known existence of magnetic loops in the solar atmosphere, it is reasonable to assume that the particles are accelerated in loops, and subsequently produce gamma rays by interacting with gas in the same loops.

In addition to this trapping argument, the observation of a greater than 10 MeV gamma-ray continuum from flares on the solar disk (Rieger 1989) provides another strong motivation for the study of loop models. For it is almost certain that this continuum emission is bremsstrahlung from ultrarelativistic electrons whose radiation pattern is highly collimated. Since it is much more likely that these electrons are accelerated in the corona rather than in the photosphere, there must exist a mechanism which reflects them and allows them to interact on their way up in the solar atmosphere. Multiple bounces between magnetic mirror points in convergent flux tubes is a viable mechanism (Ramaty *et al.* 1988).

The effect of the magnetic mirror force on the production of gamma rays in solar flares was first investigated by Zweibel and Haber (1983). These authors showed that the mirror force, acting in the convergent chromospheric magnetic fields, could prevent a large fraction of the protons accelerated isotropically in the corona from penetrating into the denser portions of the solar atmosphere. As a result, the removal time of the protons from the loops could be quite long, leading to extended time profiles of gamma-ray production which would be in conflict with the very impulsive observed profiles (e.g., Forrest 1983). Zweibel and Haber (1983) point out, however, that the problem could be solved if, in addition to the magnetic mirroring, pitch-angle scattering resulting from magnetohydrodynamic (MHD) turbulence were taken into account. Subsequently, Hua, Ramaty and Lingenfelter (1989) and Miller and Ramaty (1989), employing detailed Monte Carlo simulation, showed that this is indeed the case. By including all of the relevant physical processes in the Monte Carlo codes, they showed that the lifetime of the particles in the loop against interactions with the gas can be on the order of a few seconds, the typical decay time of gamma-ray emission in impulsive solar flares.

Closely related to this problem is the observation that gamma-ray continuum emission is preferentially observed from solar flares located at or near the limb of the Sun (Rieger *et al.* 1983; Vestrand *et al.* 1987; Rieger 1989). Dermer and Ramaty (1986) showed that this limb brightening could be understood if the gamma-ray continuum emission is bremsstrahlung produced by interacting electrons whose angular distribution contains more electrons moving in directions tangential to the photosphere than normal to it. Such electron distributions could result from transport in convergent chromospheric magnetic fields (Petrosian 1985; Kocharov *et al.* 1988; Ramaty *et al.* 1988; MacKinnon and Brown 1989;

Miller and Ramaty 1989). The Monte Carlo calculations of Miller and Ramaty (1989) have taken into account both the magnetic mirror force and MHD pitch-angle scattering. If only the magnetic mirror force is taken into account, the distribution of interacting electrons peaks in a direction which is tangential to the photosphere. In the presence of pitch-angle scattering there are still more electrons moving tangentially than are moving out from the Sun, but if the scattering is strong (to be defined below) the distribution of interacting electrons actually peaks in the direction pointing into the Sun.

In the present paper we discuss all of the above issues. We first describe the loop models and the physical processes that operate therein. Next we review the results of Monte Carlo simulations of ion and relativistic electron transport, discussing in particular depth distributions, time dependences, and angular distributions.

II. MODELS AND PHYSICAL PROCESSES

In this section we describe the salient features of the loop models for ion and relativistic electron transport in solar flares. Our discussion is based mainly on the recent papers of Hua, Ramaty, and Lingenfelter (1989), and Miller and Ramaty (1989).

a) *Loop Structure*

The model consists of a single loop or a system of essentially identical loops. Each loop has a coronal segment, in which the magnitude of the magnetic field is constant, and two subcoronal segments in which the magnetic field and gas density increase with increasing depth. The gas is fully ionized in the corona and is neutral in the subcoronal segments. The subcoronal segments are parallel to a solar radius and extend from the ends of the coronal segment at the transition region into the chormosphere and photosphere. The temperature and gas density in the corona are constant. In the subcoronal segments the gas density increases with increasing depth and the pressure is calculated from hydrostatic equilibrium. Following the prescription of Zweibel and Haber (1983), the magnetic field B is assumed to vary as a power δ of the pressure. For the atmospheric model used and $\delta = 0.2$, B increases by about an order of magnitude from the transition region to the photosphere. For larger (smaller) values of δ there will be a larger (smaller) ratio of the photospheric field to the field at the transition region.

b) *Particle Acceleration*

The particles are most likely accelerated in the corona. This is primarily because pitch-angle scattering by MHD turbulence is required for the two most commonly discussed acceleration mechanisms—viz., stochastic acceleration and diffusive shock acceleration (Forman, Ramaty, and Zweibel 1986). Such turbulence could be produced during the primary flare energy release and could exist in the ionized corona, but is expected to be quickly damped by collisions between ions and neutral atoms below the transition region. The energy spectrum, angular distribution, and time profile of the accelerated particles depend upon the acceleration mechanism. Whereas a variety of acceleration mechanisms could operate in solar flares, detailed energy spectra have so far been developed only for stochastic acceleration (Tverskoi 1967; Ramaty 1979; Barbosa 1979; Forman, Ramaty, and Zweibel 1986; Miller, Ramaty, and Murphy 1987; Miller and Ramaty 1987) and shock acceleration (Ellison and Ramaty 1985). The ion transport study of Hua, Ramaty, and Lingenfelter (1989) is based on the Bessel function spectrum appropriate for stochastic acceleration in the nonrelativistic regime, whereas the electron transport study of Miller and Ramaty (1989) uses a power law which is appropriate for both stochastic and shock acceleration in the relativistic regime.

There are no predictions of the expected angular distributions and time dependences of the accelerated particles. In most of the calculations, therefore, the particles are injected instantaneously at the top of the coronal segment with an isotropic angular distribution. A beamed distribution, however, was also considered by Hua, Ramaty, and Lingenfelter (1989).

c) *Particle Transport*

To first order, the motion of the accelerated particles throughout the loop is governed by the magnetic mirror force, whose effect can be expressed by the conservation of $(1-\mu^2)/B$, where μ is the cosine of the particle's pitch angle. In the coronal segment, where B is assumed constant, the particles move with constant pitch angle. But in the subcoronal portions, where the field increases with increasing depth, the mirror force increases (decreases) the pitch angle of a downward (upward) moving particle. Particles whose pitch angles at the transition region are large enough, reach the mirror point, are reflected and emerge back into the corona. But particles with smaller pitch angles can lose all their energy before they mirror or lose enough energy to be incapable of further gamma-ray production after they emerge from below the transition region. Such particles are effectively lost from the reservoir available for gamma-ray production. The cone containing the velocity vectors of these particles at the transition region is defined as the loss cone.

We show in Figure 1 the amount of matter (expressed in g cm^{-2}) encountered by a particle in traversing the distance from the transition region to the mirror point for various values of the magnetic field convergence parameter δ (from Miller and Ramaty 1989). The initial pitch angle μ_0 is measured at the transition region. We see that a decreasing δ produces a more gradual magnetic field convergence, and thus particles with a given μ_0 will encounter more material on the way down to the mirror point. Using the results shown in this figure, we can estimate, for various nuclear interaction products, the loss-cone half-angle α_c or its cosine μ_c. For 4.438 MeV ^{12}C nuclear de-excitation photons, we assume a typical 40 MeV proton, which will fall below the threshold for line production after traversing ~ 0.7 g cm^{-2} (Barkas and Berger 1964); for pion radiation (Murphy, Dermer, and Ramaty 1987), we assume a 1 GeV proton, for which the corresponding grammage is ~ 50 g cm^{-2}; and for greater than 10 MeV bremsstrahlung we take a 20 MeV electron, which will lose 10 MeV in ~ 2 g cm^{-2} (Berger and Seltzer 1964). Then, from Figure 1 with $\delta = 0.2$, μ_c is ~ 0.89, 0.94, and 0.91 for 4.438 MeV line production, pion production, and greater than

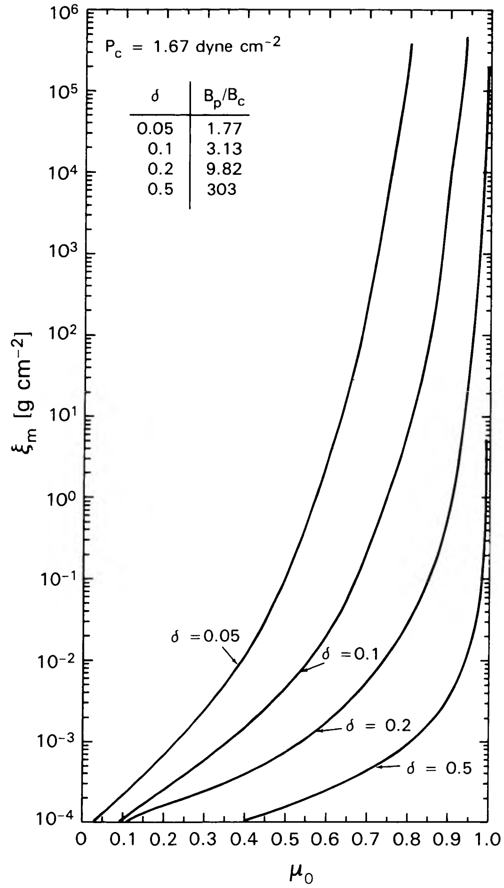

FIG. 1.—Hydrogen grammage ξ_m traversed from the transition region to the mirror point as a function of the initial pitch-angle cosine μ_0 for various δ's. P_c is the coronal pressure. (From Miller and Ramaty 1989).

10 MeV bremsstrahlung, respectively. Larger (smaller) values of μ_c, i.e., smaller (larger) loss cones, will result from larger (smaller) field convergence parameters δ.

In addition to the magnetic mirror force, the motion of the particles is also influenced by pitch-angle scattering due to MHD turbulence. As already mentioned, such turbulence is expected in the ionized corona, but not below the transition region. Whereas magnetic mirroring and losses below the transition region produce an anisotropic coronal particle distribution (the loss-cone distribution), pitch-angle scattering tends to repopulate the loss cone and hence to isotropize the particles. The distribution of the interacting particles in the subcoronal segments, where there is no pitch-angle scattering, will be anisotropic even if the particles in the corona are isotropic. The coronal distribution will become isotropic when the pitch-angle scattering rate ν exceeds the value obtained by equating the time required for particles to diffuse across the loss-cone half angle, α_c, to the transit time through the loop

$$\frac{\alpha_c^2}{\nu} \simeq \frac{2L_c}{v\langle\mu\rangle}. \tag{1}$$

Here $\langle\mu\rangle$ is the average pitch-angle cosine for a particle in the loss cone, L_c is the loop half-length, and v is the particle speed. We shall refer to this regime of pitch-angle scattering as the strong or saturated regime (see also Kennel and Petschek 1966; Kennel 1969).

Using formulae given by Miller and Ramaty (1989), we can express the scattering rate ν in terms of the energy density in the turbulence. We find that for Alfvén turbulence with a Kolmogorov spectrum and a coronal magnetic field of 100 G, ν is $\sim 50W_a$ s^{-1} for 40 MeV protons, $85W_a$ s^{-1} for 1 GeV protons and $430W_a$ s^{-1} for 20 MeV electrons. Here W_a is the energy density in Alfvén turbulence measured in ergs cm^{-3}. Then, using equation (1) and the values of μ_c obtained above (which are valid for $\delta = 0.2$), we find that both the 4.438 line emission and the pion radiation will reach saturation when the turbulent energy density exceeds $\sim 10^{-2}$ ergs cm^{-3}, while the greater than 10 MeV bremsstrahlung will saturate at an energy density of $\sim 5\times10^{-3}$ ergs cm^{-3}. The pitch-angle scattering rate can also be expressed in terms of the scattering mean free path, Λ, as was done by Hua, Ramaty, and Lingenfelter (1989) using the formalism developed by Palmer and Jokipii (1981). In terms of Λ, the scattering rate is given by $\nu = 2.4v/\Lambda$ (see formulae in Hua, Ramaty, and Lingenfelter 1989; Miller and Ramaty 1989). Then for $\mu_c = 0.89$ and $\langle\mu\rangle \simeq 0.92$ (valid for 4.438 MeV line emission, which is the emission treated by Hua, Ramaty, and Lingenfelter (1989), equation (1) implies that saturation should occur when $\lambda \equiv \Lambda/L_c \simeq 25$. In § III*b* we shall discuss the implications of saturation on the time profiles of the various emissions.

An energy density of 10^{-2} ergs cm^{-3} is less than 1% of the energy density of a few ergs cm^{-3} that is needed to accelerate protons to the GeV energies implied by observations of pion decay radiation (see Ramaty, Dennis, and Emslie 1988 for review). The turbulence which scatters the particles could therefore be the remnant of the turbulence generated by the primary energy release (e.g., magnetic reconnection) which presumably accelerated the particles. But it is important to note that MHD turbulence can also be excited by anisotropies occurring in the accelerated particle distributions. The loss-cone anisotropy is especially relevant since protons with a loss-cone distribution can excite Alfvén waves and electrons with such a distribution can excite whistlers (Wentzel 1976; Bespalov, Zaitsev, and Stepanov 1987). Effective MHD pitch-angle scattering, therefore, could occur even if there are no sources of external turbulence.

III. RESULTS OF MONTE CARLO SIMULATIONS

In this section we discuss numerical results and their implications on the location of the interaction region, on the attenuation of the gamma-ray lines, on time dependencies, and on the angular distribution of greater than 10 MeV bremsstrahlung. We also discuss the implications of saturated MHD pitch-angle scattering on models for the 1982 June 3 flare.

a) *Location of the Interaction Region and Attenuation of Gamma-Ray Lines*

The location of the interaction region depends critically on the parameters of the loop model, in particular the convergence parameter δ and the pitch-angle scattering rate, characterized by either the mean free path λ or the energy density W_a. In principle, this location could be determined from imaging observations, which could then constrain the models, but such observations are not yet available. Indirect arguments (for a review, see Ramaty, Dennis, and Emslie 1988) suggest that the interaction region could extend from below a height where the density is $\sim 10^{12}$ cm^{-3} to a depth where the density is $\sim 10^{16}$ cm^{-3}. As we shall now see, this conclusion is in good agreement with the results of the numerical calculations.

We illustrate the predictions of the model by presenting results from the calculations of Hua, Ramaty, and Lingenfelter (1989) of the depth distribution of the production of the 4.438 MeV ^{12}C nuclear deexcitation line. Figure 2 shows the effects of the convergence of the subcoronal magnetic field in the absence of pitch-angle scattering. In both this figure and Figure 3, $Q(<-1800\ \text{km})/Q_{\text{Total}}$ represents the fraction of the total line production occurring in the corona. The location of the transition region is set at -1800 km. As can be seen, except for values of δ close to zero, the gamma rays are produced predominantly in the chromosphere and corona. This is the direct consequence of the mirror force, which prevents the bulk of the particles from penetrating lower into the atmosphere. But the addition of pitch-angle scattering

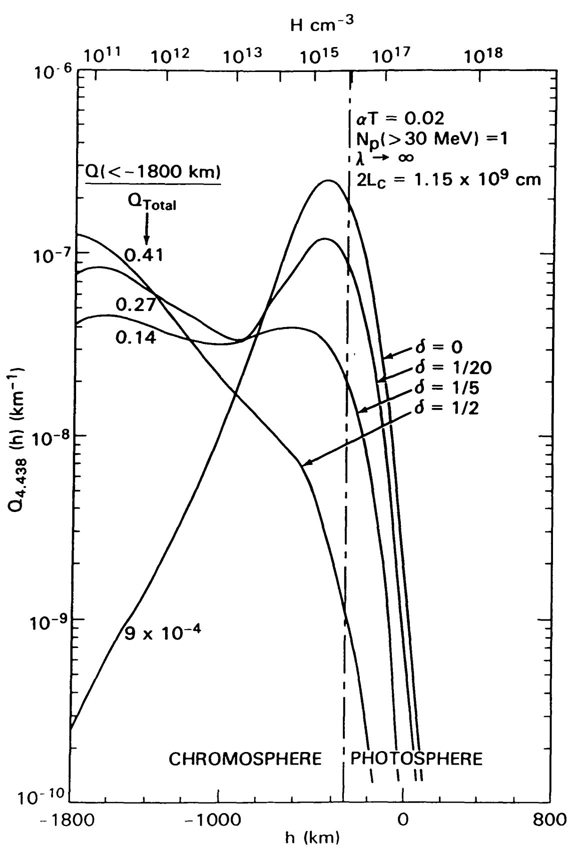

FIG. 2.—Depth distributions of the 4.438 MeV line production in magnetic fields with various values of the magnetic field convergence parameter δ in the absence of pitch-angle scattering. (From Hua, Ramaty, and Lingenfelter 1989.)

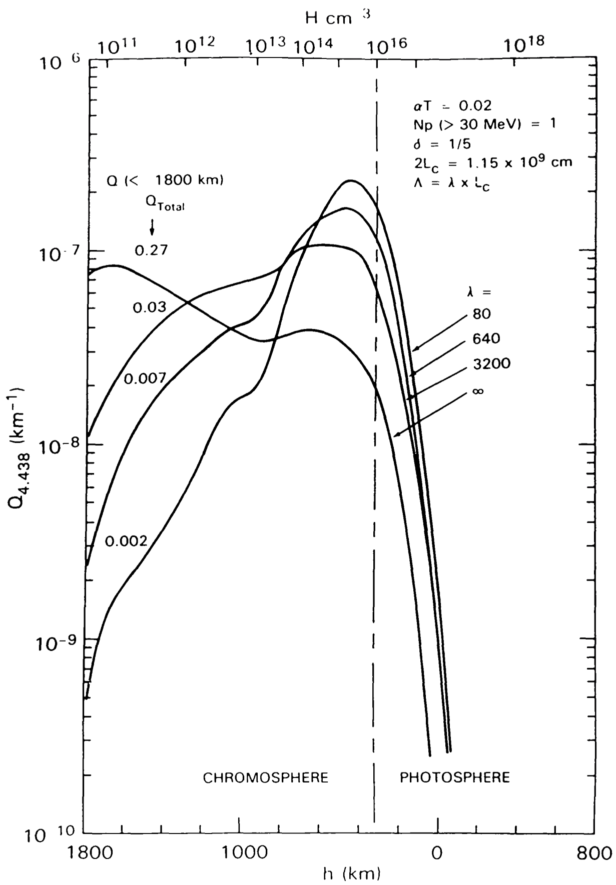

FIG. 3.—Depth distributions of the 4.438 MeV line production in a magnetic field with fixed δ in the presence of pitch-angle scattering with various mean free paths. (From Hua, Ramaty, and Lingenfelter 1989.)

moves the interaction region significantly deeper (see Fig. 3). In this case, particles with large pitch angles, which without scattering would mirror high in the atmosphere, are scattered to small pitch angles and hence produce gamma rays at much larger depths. For $\lambda = 80$, for which the transport is nearly saturated (see next section), the production peaks at ~ 150 km above the photosphere, with essentially no contribution from the corona and upper chromosphere. In fact, this depth distribution is quite similar to that corresponding to $\delta = 0$ (compare Figs. 2 and 3), indicating that in the presence of saturated pitch-angle scattering the ions are capable of penetrating to essentially the same depths that they would penetrate in the absence of magnetic field convergence.

The calculated depth profiles can be used to evaluate the attenuation of the line photons as they escape from the solar atmosphere. The dominant attenuation mechanism is Compton scattering. According to Hua, Ramaty, and Lingenfelter (1989), for a flare on the limb and with saturated pitch-angle scattering (which maximizes the interaction depth and hence the attenuation), the fraction of the photons that escape from the solar atmosphere without Compton scattering is ~ 0.75, 0.70, 0.70, and 0.63 for the 6.129, 4.438, 1.63, and 0.847 MeV lines, respectively. These escape fractions approach unity if the heliocentric angle of the flare is less than 85°, but they decrease rapidly for angles greater than 90°. Hua, Ramaty, and Lingenfelter (1989) showed that no significant modifications due to line attenuation are necessary for the abundance results obtained by Murphy *et al.* (1985*a*, *b*) for the 1981 April 27 flare (88°W, 16°N).

Stronger attenuation, however, is expected for lower energy lines. From calculations whose results we report here, we found that the escape fraction for the ~ 0.45 MeV line from $\alpha - \alpha$ reactions (Kozlovsky and Ramaty 1974) is only $\cong 0.4$ for a limb flare with saturated pitch-angle scattering (see also Murphy *et al.* 1990). Furthermore, we would expect an even lower escape fraction for the 0.511 MeV positron annihilation line, because the positrons emitters, on the average, are produced by higher energy ions, which penetrate deeper than the α particles which produce the ~ 0.45 MeV line. (For a detailed treatment of positron-emitter production see Kozlovsky, Lingenfelter, and Ramaty 1987). But the depth distribution of the production of positron emitters and the transport of the resultant positrons, has not yet been studied.

b) *Time Dependences and the Need for MHD Pitch-Angle Scattering*

The same considerations which enter into our discussion of the depth profiles area also relevant to the study of the time dependences. These are illustrated in Figure 4 (from Hua, Ramaty, and Lingenfelter 1989) which shows the effects of a varying mean free path λ on the time dependence of the production of the 4.438 MeV line. The quantity

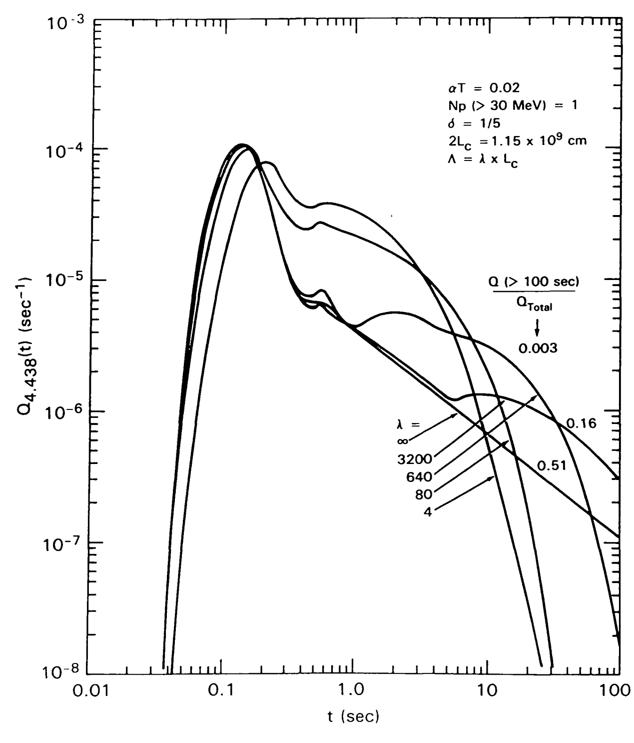

FIG. 4.—Time dependence of the 4.438 MeV line production in a magnetic field with fixed δ in the presence of pitch-angle scattering with various mean free paths. (From Hua, Ramaty, and Lingenfelter 1989.)

$Q(>100\ \mathrm{s})/Q_{\mathrm{total}}$ represents the fraction of the line photons produced after the first 100 s. In the calculations, the ions were released instantaneously and isotropically at the top of a loop. If there is no scattering ($\lambda \to \infty$), there is an initial spike of radiation, produced by ions in the loss cone, followed by extended emission due to ions trapped between mirror points high in the chromosphere. These ions spend most of their time in the corona. The extended time profile resulting from this trapping, with approximately half of the emission appearing after 100 s is clearly inconsistent with the observed time profiles of nuclear gamma rays observed from impulsive solar flares (e.g., the 1981 June 21 flare; Forrest 1983).

But as expected, by decreasing λ the time profiles in Figure 4 become much less extended. This is because the trapped ions with large pitch angles are scattered into the loss cone on much shorter time scales than the ion removal time from the corona by nuclear interactions, Coulomb energy losses or drifts. (For an estimate of the drift time scale see Ramaty *et al.* 1988.) Saturation is indeed approached around $\lambda = 25$, as there is not much difference between the time profiles corresponding to $\lambda = 80$ and $\lambda = 4$. When saturation occurs, the time profiles become independent of the pitch-angle scattering rate, but they still depend on the loop length and on the convergence parameter δ. Hua, Ramaty, and Lingenfelter (1989) showed that if the decaying portions of the time profiles of the 4.438 MeV line flux are approximated by exponentials with characteristic time τ, then in the saturated regime for $\delta = 0.2$, $\tau = 3.5\mathrm{s}(L_c/10^9)$.

A simple estimate of τ at saturation, which shows the dependence on δ and is valid also for other emissions, is given by

$$\tau \simeq 2L_c/[v\langle\mu\rangle(1-\mu_c)], \tag{2}$$

(Zweibel and Haber 1983; Hua, Ramaty and Lingenfelter 1989; Miller and Ramaty 1989). Using the values of μ_c obtained in § II*c* for the 4.438 MeV line emission, pion radiation, and greater than 10 MeV bremsstrahlung, and taking proton velocities at 20 MeV for nuclear line production and 700 MeV for pion production, we obtain that $\tau/(L_c/10^9\ \mathrm{cm})$ is ~ 3.2, 1.4, and 0.8 s, for the three types of emission, respectively. These values are again valid for $\delta = 0.2$. For other values of δ, equation (2) can be evaluated by using the appropriate loss-cone cosines, μ_c, which can be derived from the results shown in Figure 1. Larger (smaller) field convergence parameters δ will produce larger (smaller) values of τ.

We see that the estimate for the 4.438 MeV emission given by equation (2) is in reasonable agreement with the value obtained from the Monte Carlo simulations. But we also note that, at saturation, the time scale for pion radiation is very short, actually somewhat shorter than that for the 4.438 MeV line emission, primarily because the protons which produce pions have higher velocities than those which produce the 4.438 MeV line photons. This is quite different from the situation in which pitch-angle scattering is not taken into account. It has been shown that in a loop model with convergent magnetic field but no pitch-angle scattering, the time scale of the pion radiation is much longer than that of the nuclear line emission (Kocharov *et al.* 1988). This is because without pitch-angle scattering, as we have seen, the bulk of the ions mirror high in the chromosphere and therefore traverse only a very small amount of matter in each bounce between mirror points. Therefore, to traverse the ~ 50 g cm^{-2} of matter needed to produce pions, a much larger number of bounces is required than the number needed to traverse the ~ 0.7 g cm^{-2} for nuclear line production. On the other hand, when pitch-angle scattering is added, the bulk of the particles interact in the loss cone. Therefore, the time scale is determined, not by the number of bounces needed to traverse a given amount of matter—which is vastly different for nuclear line and pion production, but by the scattering rate into the loss cone—which is not very different for the nuclear-line–producing and pion-producing protons.

c) *Models for the 1982 June 3 Flare*

The above results have important implications for the 1982 June 3 flare from which pion radiation has been observed (Forrest *et al.* 1985, 1986). The time profiles of the nuclear line emission and the pion radiation from this flare are shown in Figure 5 (from Ramaty, Murphy, and Dermer 1987, based on data from Forrest *et al.* 1986 and Chupp *et al.* 1987). As has been emphasized by Murphy, Dermer, and Ramaty (1987), the fact that the ratio of the flux in pion emission to that in nuclear-line emission is much larger during the second pulse than during the first, indicates that the spectrum of the interacting protons became harder with time during the flare. Murphy, Dermer, and Ramaty (1987) proposed that this hardening was due to second-phase acceleration. Their model did not incorporate magnetic loops, so that in our present discussion their calculations would correspond to the case of no magnetic field convergence, i.e., $\delta = 0$. In this case there is not much delay between the particle acceleration and interaction. Therefore, the fact that during the first pulse the interacting particles had a steeper spectrum than those interacting during the second pulse must mean different accelerated proton spectra for the two pulses. This is the origin of the second phase suggestion for this flare.

On the other hand, Kocharov *et al.* (1988) suggested that the difference between the two time profiles resulted from the longer time scale of the pion emission expected in loop models without pitch-angle scattering. Specifically, in the Kocharov *et al.* (1988) model, there is no pitch-angle scattering until the onset of the second pulse (~120 s after 11:42:11 UT; see Fig. 5). As a result, the pion radiation observed in the first pulse is due mainly to the GeV protons in the loss cone. Thus, since isotropy is assumed in the model, the bulk of the GeV protons remain trapped in the corona and available for pion production at later times. Pitch-angle scattering is turned on at the onset of the second pulse by the introduction of an external source of turbulence. This causes the rapid dumping of all the trapped particles. But because of their shorter loss time in the absence of pitch-angle scattering, not too many low energy protons remain at this time. In the resultant second pulse, therefore, pion radiation dominates.

It is probably unlikely that pitch-angle scattering is negligible during the first pulse. It has been shown (Hua, Ramaty, and Lingenfelter 1989; Miller and Ramaty 1989) that the decaying portions of the time profiles of both the nuclear line

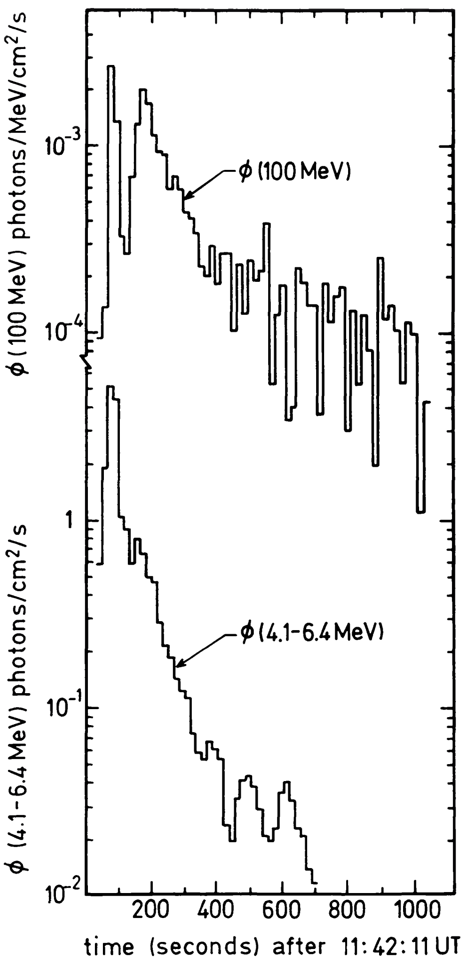

FIG. 5.—Time profiles of the pion decay radiation, ϕ(100 MeV), and nuclear line emission, ϕ(4.1–6.4 MeV) observed from the 1982 June 3 flare. (From Ramaty, Murphy, and Dermer 1987, based on data of Forrest *et al.* 1986 and Chupp *et al.* 1987.)

emission and the greater than 10 MeV bremsstrahlung observed from the 1980 June 21 flare (Forrest 1983) can be well fitted in a loop model with pitch-angle scattering close to saturation, and there is no reason to believe that the 1982 June 3 flare would be different in this respect from the 1980 June 21 event. Furthermore, as we have mentioned in § II*c*, even in the absence of external sources of turbulence, pitch-angle scattering could occur as a result of turbulence generated by the electromagnetic loss-cone instability. A viable model for the 1982 June 3 flare, therefore, would have to be based on different accelerated particle spectra for the two pulses, as suggested by Murphy, Dermer, and Ramaty (1987), and not on the prolonged trapping of high-energy protons in the loop, as suggested by Kocharov *et al.* (1988).

d) *Angular Distributions of Greater than 10 MeV Bremsstrahlung*

Angular distributions for bremsstrahlung production in loop models with converging subcoronal magnetic fields have been calculated by Semukhin and Kovaltsov (1985), Kocharov

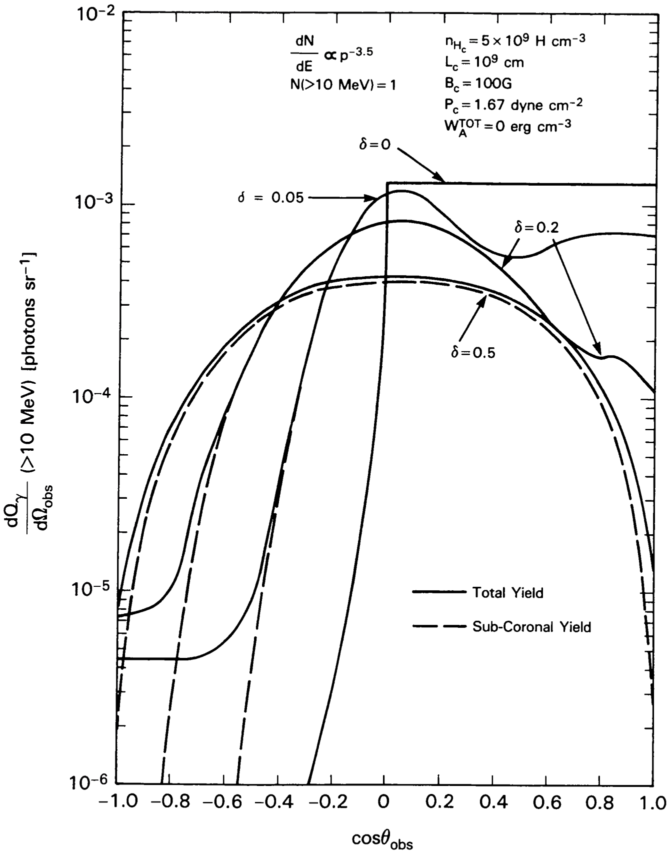

FIG. 6.—Angular distributions of greater than 10 MeV bremsstrahlung for various values of δ. The observation angle $\theta_{\rm obs}$ is the angle between a downward-directed solar radius vector and the direction of observation. Negative values of $\cos(\theta_{\rm obs})$ correspond to the upward hemisphere. Coronal MHD turbulence is absent. (From Miller and Ramaty 1989).

et al. (1988), Ramaty *et al.* (1988), MacKinnon and Brown (1989), and Miller and Ramaty (1989). In Figure 6 (from Miller and Ramaty 1989) we show angular distributions of greater than 10 MeV bremsstrahlung in a loop model with various values of δ and no pitch-angle scattering. Here $\theta_{\rm obs}$ is the angle between the direction of observation and a downward-directed solar radius. Both the total and the subcoronal bremsstrahlung yields are shown.

If the magnetic field is not converging ($\delta = 0$), there is no process by which the pitch angle of an electron can be changed after injection. Therefore, the resulting bremsstrahlung distribution is virtually isotropic in the downward hemisphere and falls off very rapidly in the backward hemisphere, where any emission is due to the angular spread of the bremsstrahlung. However, if the magnetic field converges and δ is not too small, there is almost as much radiation in the upward hemisphere as in the downward one, and the angular distributions peak at $\theta_{\rm obs} = 90°$. The radiation at $\cos\theta_{\rm obs}$ close to 1 is due to electrons with pitch angles in the loss cone which interact before they mirror.

There are at present 15 solar flares from which greater than 10 MeV emission has been observed (Rieger 1989). Of this number, 13 (or $\approx 87\%$) have heliocentric longitudes $l \gtrsim 64°$. This strongly indicates that the greater than 10 MeV emission is anisotropic, with more emission in directions tangential to the photosphere than normal to it. If the emission were isotropic, this fraction would only be $\approx 29\%$. However, of the two flares with $l < 64°$, one flare (1984 April 25) is located on the disk at E43°, S12°, and exhibits strong bremsstrahlung emission at energies greater than 25 MeV (E. Rieger, private communication, 1988). Thus, even though the observable angular distribution should peak at directions tangential to the photosphere, there also should be significant emission in the backward hemisphere.

The angular distribution for the $\delta = 0$ falls off far too rapidly in the hemisphere away from the Sun to account for emission greater than 10 MeV from flares with $l \lesssim 80°$, since at these longitudes the emission is less than 1% of that at 90°. In particular, the $\delta = 0$ distribution would be inconsistent with the observations of the 1984 April 25 flare, whose position is far removed from the limb. On the other hand, the distribution for $\delta = 0.2$ produces significant radiation at $\cos\theta_{\rm obs} = -0.71$, which could account for the 1984 April 25 flare. It is this result that provides one of the strongest indications for the validity of loop models with convergent subcoronal magnetic fields. Unless the field converges, there is no mechanism for producing ultrarelativistic bremsstrahlung in directions away from the Sun (except if the angle between the loop axis and a solar radius is much larger than 0).

The $\delta = 0.2$ curve, coupled with a reasonable flare size distribution (Dermer and Ramaty 1986; Miller and Ramaty 1989), can also produce a longitude distribution of greater than 10 MeV–emitting flares which fits the distribution of the 15 observed flares quite well. Much larger values of δ would imply unreasonably large photospheric magnetic fields and would ultimately produce longitude distributions which are inconsistent with the observations. Values of δ close to 0, as already pointed out, would not produce enough ultrarelativistic bremsstrahlung for flares on the disk.

The effects of pitch-angle scattering on the angular distribution of greater than 10 MeV bremsstrahlung are shown in Figure 7 (from Miller and Ramaty 1989), for various values of the energy density in Alfvén turbulence. As can be seen, as W_a is increased, the distribution increasingly peaks in the downward direction. This is because electrons, which would otherwise mirror in the chromosphere and produce most of their radiation at $\theta = 90°$, are now scattered into smaller pitch angles, whose corresponding mirror heights are within the photosphere. Many of these electrons have insufficient energy to reach these new mirror points, and so interact on the way down, where they enhance the downward- directed radiation. At an energy density of $W_a = 2 \times 10^{-2}$ ergs cm^{-3} the greater than 10 MeV bremsstrahlung is saturated for $L_c = 10^9$ cm and $\delta = 0.2$ (see § III*b*). In this regime, the angular distribution actually peaks in the downward direction.

By comparing the $\delta = 0.2$ curve in Figure 6 with any one of the curves in Figure 7, we see that in the upward hemisphere there is not much difference between the shapes of the distributions with or without pitch-angle scattering. While the curves in the downward hemisphere are quite different, photons emitted into these directions, of course, cannot be observed. It follows, therefore, that observations of the angular

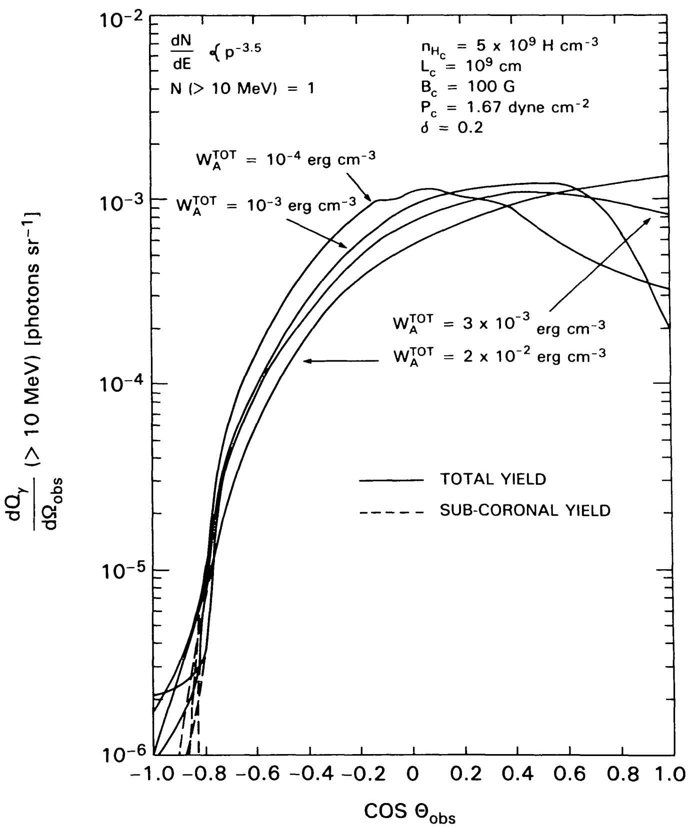

FIG. 7.—The angular distributions of the greater than 10 MeV bremsstrahlung for various values of W_a. The $W_a = 2\times10^{-2}$ erg cm^{-3} curve corresponds to saturation, and $\theta_{\rm obs}$ is defined in the previous figure. (From Miller and Ramaty 1989).

distribution of the gamma-ray continuum cannot serve as a diagnostic for the presence of pitch-angle scattering. On the other hand, the shapes of nuclear de-excitation gamma-ray lines are sensitive to the entire energetic particle angular distribution and not just to that portion of the distribution which contains particles radiating toward the observer. Particularly promising in this respect are the 0.429 and 0.478 MeV lines resulting from the interactions of accelerated α particles with ambient helium (Murphy, Kozlovsky, and Ramaty 1988). Calculations of the shapes of these lines and their dependence on the parameters of the loop model have recently been completed (Murphy *et al.* 1990).

IV. SUMMARY

We have reviewed the motivations for considering magnetic loop models for ion and relativistic electron transport in solar flares, the physical processes that operate in the loops, and numerical results for nuclear line and ultrarelativistic bremsstrahlung production in the loops. We find that magnetic mirroring provides a good explanation both for the production of ultrarelativistic bremsstrahlung from flares on the disk and for the preferential detection of greater than 10 MeV continuum emission from flare close to the limb. We also find that in loop models with mirroring, MHD pitch-angle scattering is required to prevent the trapping of the particles in the corona for long time periods; such trapping would be inconsistent with the observations. We show that when MHD pitch-angle scattering is taken into account, it is unlikely that the very different time profiles of pion radiation and nuclear line emission observed from the 1982 June 3 flare were caused by transport. We suggest that separate acceleration phases are required, as was proposed previously.

R. R. wishes to acknowledge the hospitality of Monique Pick at the Observatoire de Paris in Meudon where part of this paper was completed. We also acknowledge the following funding supports: NASA Graduate Student Fellowship Grant NGT-50055 for J. A. M., NASA Grant NGR-21-002-316 for X. M. H. and NSF grant ATM 8717676 for R. E. L.

REFERENCES

Barbosa, D. D. 1979, *Ap. J.*, **233**, 383.
Barkas, W. H., and Berger, M. J. 1964, NASA SP-3013, *Tables of Energy Losses and Ranges of Heavy Charged Particles*, (Washington, DC: NASA).
Berger, M. J., and Seltzer, S. M. 1964, NASA SP-3012, *Tables of Energy Losses and Ranges of Electrons and Positrons*, (Washington, DC: NASA).
Bespalov, P. A., Zaitsev, V. V., and Stepanov, A. V. 1987, *Solar Phys.*, **114**, 127.
Chupp, E. L. 1984, *Ann. Rev. Astr. Ap.*, **22**, 359.
______. 1987, *Phys. Scripta*, **T18**, 5.
Chupp, E. L., *et al.*, 1987, *Ap. J.*, **318**, 913.
Dermer, C. D., and Ramaty, R. 1986, *Ap. J.*, **301**, 962.
Ellison, D. C., and Ramaty, R. 1985, *Ap. J.*, **298**, 962.
Forman, M. A., Ramaty, R., and Zweibel, E. G. 1986, in *The Physics of the Sun*, ed. P. A. Sturrock, Vol. **2** (Dordrecht: Reidel), p. 249.
Forrest, D. J. 1983, in *Positron and Electron Pairs in Astrophysics*, ed. M. L. Burns, A. K. Harding, and R. Ramaty (New York: AIP), p. 3.
Forrest, D. J., Vestrand, W. T., Chupp, E. L., Rieger, E., Cooper, J., and Share, G. 1985, *19th Internat. Cosmic Ray Conf.*, **4**, 146.
Forrest, D. J., Vestrand, W. T., Chupp, E. L., Reiger, E., Cooper, J., and Share, G. 1986, *Adv. Space Res.*, **6**, No. 6, 115.
Hua, X.-M., Ramaty, R., and Lingenfelter, R. E. 1989, *Ap. J.*, **341**, 516.
Kennel, C. F. 1969, *Rev. Geophys.*, **7**, 379.
Kennel, C. F., and Petschek, H. E. 1966, *J. Geophys. Res.*, **71**, 1.
Kocharov, G. E., Kocharov, L. G., Kovaltsov, G. A., and Mandzhavidze, N. Z. 1988, preprint.
Kocharov, G. E., Kovaltsov, G. A., Mandzhavidze, N. Z., Semukhin, P. E., and Kocharov, L. G. 1987, *20th Internat. Cosmic Ray Conf.*, **3**, 74.
Kozlovsky, B., Lingenfelter, R. E., and Ramaty, R. 1987, *Ap. J.*, **316**, 801.
Kozlovsky, B., and Ramaty, R. 1974, *Ap. J. (Letters)*, **191**, L43.
MacKinnon, A. L., and Brown, J. C. 1989, *Astr. Ap.*, **215**, 371.
Miller, J. A., and Ramaty, R. 1987, *Solar Phys.*, **113**, 195.
______. 1989, *Ap. J.*, **344**, 973.
Miller, J. A., Ramaty, R., and Murphy, R. J. 1987, *20th Internat. Cosmic Ray Conf.*, **3**, 33.
Murphy, R. J., Dermer, C. D., and Ramaty, R. 1987, *Ap. J. Suppl.*, **63**, 721.
Murphy, R. J., Hua, X.-M., Kozlovsky, B., and Ramaty, R. 1990, *Ap. J.*, **351**, 299.
Murphy, R. J., Forrest, D. J., Ramaty, R., and Kozlovsky, B. 1985*a*, *19th Internat. Cosmic Ray Conf.*, **4**, 253.
Murphy, R. J., and Ramaty, R. 1984, *Adv. Space Res.*, **4**, No. 7, p. 127.
Murphy, R. J., Ramaty, R., Forrest, D. J., and Kozlovsky, B. 1985*b*, *19th Internat. Cosmic Ray Conf.* **4**, 249.
Palmer, I. D. and Jokipii, J. R. 1981, *17th Internat. Cosmic Ray Conf.*, **3**, 381.
Petrosian, V. 1985, *Ap. J.*, **299**, 987.

Ramaty, R. 1979, in *Particle Acceleration Mechanisms in Astrophysics*, ed. J. Arons, C. Max, and C. McKee (New York: AIP), p. 135.
Ramaty, R., Dennis, B. R., and Emslie, A. G. 1988, *Solar Phys.*, **118**, 17.
Ramaty, R., Miller, J. A., Hua, X.-M., and Lingenfelter, R. E. 1988, in *Nuclear Spectroscopy of Astrophysical Sources*, ed. N. Gehrels and G.H. Share (New York: AIP), p. 217.
Ramaty, R., and Murphy, R. J. 1987, *Space Sci. Rev.*, **45**, 213.
Ramaty, R., Murphy, R. J., and Dermer, C. D. 1987, *Ap. J. (Letters)*, **316**, L41.
Rieger, E. 1989, *Solar Phys.*, **121**, 323.
Rieger, E., Reppin, C., Kanbach, G., Forrest, D. J., Chupp, E. L., and Share, G. H. 1983, *18th Internat. Cosmic Ray Conf.*, **10**, 338.
Semukhin, P. E., and Kovaltsov, G. A. 1985, *19th Internat. Cosmic Ray Conf.*, **4**, 106.
Tverskoi, B. A. 1967, *Soviet Phys., JETP*, **25**, 317.
Vestrand, W. T., Forrest, D. J., Chupp, E. L., Rieger, E., and Share, G. H. 1987, *Ap. J.*, **322**, 1010.
von Rosenvinge, T. T., Ramaty, R. and Reames, D. V. 1981, *17th Internat. Cosmic Ray Conf.*, **3**, 28.
Wentzel, D. G. 1976, *Ap. J.*, **208**, 595.
Zweibel, E. G., and Haber, D. 1983, *Ap. J.*, **264**, 648.

X.-M. Hua: Space Astrophysics Lab/ISTS, 2700 Steeles Avenue West, Concord, Ontario, Canada L4K 3C8

R. E. Lingenfelter: Center for Astrophysics and Space Sciences, University of California, San Diego, CA 92093

J. A. Miller and R. Ramaty: Code 665, Laboratory for High Energy Astrophysics, Goddard Space Flight Center, Greenbelt, MD 20771